DOI: 10.17277/amt.2019.03.pp.008-015

Raman Spectroscopy and Crystalline Structure of Polyacrylonitrile-Based Carbon Fibres

V.M. Samoilov*, V.B. Samsonova, A.V. Nakhodnova, D.B. Verbets, A.R. Gareev, I.A. Bubnenkov, N.N. Steparyova, A.A. Shvetsov, N.G. Bardin

JSC "Scientific research Institute of structural materials based on graphite "NIIgrafit",
2, ul. Electrode, Moscow, 111524, Russia

*Corresponding author. Tel.: +7 916 608 96 49. *E-mail*: vsamoylov@niigrafit.org

Abstract

PAN-based carbon fibres (**CFs**) processed at temperatures from 1000 to 3000 °C were studied with the Raman spectroscopy and X-ray diffraction methods. It is shown that the I_D/I_G parameter (the ratio of the integral intensities of the D and G spectral bands) measured on the surface of CFs decreases with the increase of heat treatment temperature, alongside with an increase of crystallite sizes L_a and L_c and a decrease of interlayer spacing d_{002}.

In addition, the I_D/I_G parameter was measured on longitudinal and transverse cross-sections of the same CF samples. The Tuinstra-Koenig relation was used to obtain the corresponding crystallite sizes L_a. It is shown that the crystalline structure of high-strength CFs had a high degree of heterogeneity. On the other hand, filaments of high-modulus PAN-based CFs contained maximal size crystals on the periphery and minimal size crystals in the center.

Relations between the crystallite sizes were determined using the Raman spectroscopy method and measured on the surface, and the transverse cross-section of CF filaments and the heat treatment temperature were found. It is shown that the growth speed of crystallites at a graphitization temperature in the interval 2500–3000 °C was approximately 5 times higher on the periphery than in the centre of filaments. The obtained data were an independent validation of the structural model of Bennett and Johnson for PAN-based CFs.

Keywords

Carbon fibre; PAN-based fibre; crystalline structure; graphitization; raman spectroscopy; X-ray diffraction.

Introduction

In recent decades, carbon fibers (**CFs**) on the basis of polyacrylonitrile (**PAN**), mesophase pitch, and cellulose have become materials determining the scientific and technological advancement in the space industry, aircraft construction, wind power engineering, and hydrogen power engineering [1–4]. At present, high-modulus CFs are widely applied in the automotive industry, production of high-quality sporting equipment, medicine, construction engineering, etc. [3, 4].

The world's market is dominated by PAN-based CFs. Modern high-modulus CFs are synthesized from the source PAN fibers by using a continuous technological process in relatively long lines, successively carrying out several thermal processing stages, namely, thermal stabilization (180–270 °C), carbonization (700–1500 °C), and graphitization (2200–3000 °C) [1–4]. It is widely accepted that the crystalline structure transformation processes occurring at temperatures 1000–3000 °C play a crucial role in the formation of the physical and mechanical properties of the obtained CFs [1–5].

Raman spectroscopy is one of the most highly sensitive methods capable of probing the crystalline structure of carbon materials [6–8]. However, in the past years this method was mostly used in investigating and identifying nanocarbon materials, such as graphene, carbon nanotubes and their derivatives [9, 10]. Raman spectroscopy was also used in the study

of the crystalline structure of CFs [11–13]. However in most cases, Raman spectra are presented for particular CF brands, without reference to the specific technological production process parameters.

The aim of this investigation was to study the parameters of Raman spectroscopy of high-modulus and high-strength PAN-based CF samples processed at different heat treatment temperatures (**HTT**), as well as to analyze the possibility of the use of Raman spectroscopy as a structure-sensitive method in the development of perspective technological processes for obtaining high quality CFs. Special attention was payed to the use of Raman spectroscopy as a method for the analysis of heterogeneity of the crystalline structure of CFs, a property problematic to study with the use of the X-ray diffraction and electron microscopy methods.

Materials and methods

A standard high-strength CF of the T-700 brand (Torayca) with a density of 1.78 g/cm^3, an average diameter of filaments from 6.3 to 6.5 μm, a tensile strength of 5.2 GPa, and a Young modulus of 231 GPa was used as a starting CF. The thermal treatment (graphitization) of the starting CF was carried out in an LPU-1 experimental line developed in AO NIIgrafit. The high-temperature thermal processing was carried out in a modernized Tamman furnace mounted in a cooled steel casing under an argon atmosphere. A tube graphite heater of special design was used which provided a 186 mm operating part of the high-temperature heating zone (2500–3000 °C). The fiber was pulled out using feeding and receiving mechanisms, such as a feeding creel, pickup device, and transmitting drum tension levelers. The winding rate was adjusted using a frequency converter, and the tension was measured by a strain gauge. The temperature was measured by a TUBE-66 optical pyrometer and tungsten–rhenium thermocouple. The pulling off and the load on the thermally processed carbon filament with a linear density of 810 tex, were implemented by changing the speeds of feeding and receiving mechanisms. The load was 20 MPa on average. The CF series was obtained at processing temperatures from 1290 to 3000 °C with a pulling speed of 10 m/h.

The degree of perfection of the crystalline structure and the homogeneity of high-modulus CFs were studied via the method of Raman spectroscopy. The measurements were carried out both on the surface of samples of individual CF filaments and on samples of longitudinal sections of thin CF filaments (Fig. 1*a*, *b*).

The Raman spectra were recorded in the broad spectral range of 700–3000 cm^{-1} using a Renishaw in Via Reflex confocal Raman microspectrometer. The micro spectrometer was equipped with an optical microscope and a cooled CCD detector. The laser beam was focused to a spot of approximately 0.5 μm in diameter by a 100x microscope objective. The laser radiation power was 1 mW. The excitation radiation of a Nd:YAG solid-state diode-pumped laser had a wavelength of 532 nm. Carbon materials, including CFs, usually show two characteristic bands in the first-order spectrum (1000–2000 cm^{-1}) [9–12].

One of them is an allowed Raman scattering band at 1580 cm^{-1}, which corresponds to an ideal graphite vibration mode with the E_{2g} symmetry and is often called the G mode [10–13]. The G band is determined by the oscillations of carbon atoms in the plane of the graphene layers and is associated with carbon atoms in the sp^2 hybridization state. Another active Raman scattering band at 1360 cm^{-1} is induced by unordered carbon atoms and corresponds to lattice vibrations with the A_{1g} symmetry and is called the D mode [10–13]. The D band is associated with carbon atoms in the sp^2 and sp^3 hybridization states, which are localized in the area of defects and on the periphery of graphene layers [11–13]. The D band is absent in single-crystal graphite, and an increase in its intensity is considered to be a result of an increase in the amount of disordered carbon [11–13].

According to the results of numerous studies, the ratio of the integral intensities of these bands, i.e., the I_D/I_G parameter, at crystallite sizes of more than 2 nm [10–13] is determined by the average distances between defects and allows one to characterize the average lateral dimensions L_a of the crystallite for carbon materials at the stage of graphitization from the following formula [7, 10–13]:

$$\frac{I_D}{I_G} = \frac{C(\lambda)}{L_a}, \qquad (1)$$

where $C(\lambda)$ is the constant depending on the wavelength and energy of laser radiation; the C (λ = 514 nm) value is approximately equal to 4.4 nm [12].

The X-ray diffraction phase and structure analysis of high-modulus CFs were carried out on a DIFREY-401 X-ray diffractometer equipped with a sharp-focus X-ray tube with a cobalt (Co) anode, a curved coordinate-sensitive detector, and a system for simultaneous recording of the X-ray diffraction pattern in a large range of angles. The $K\alpha$ series of X-ray

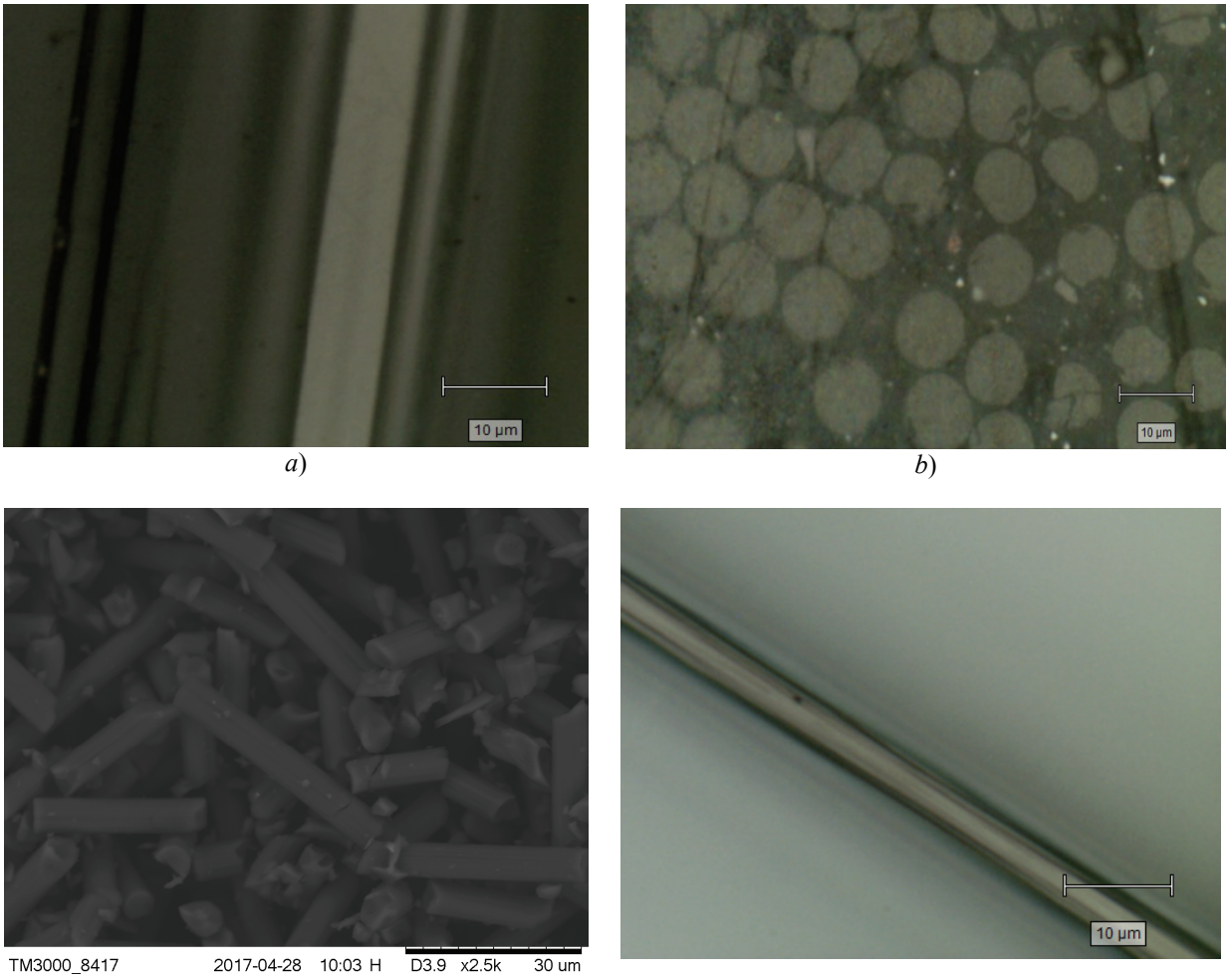

a) *b*)

c) *d*)

Fig. 1. An optical microscopy image of the longitudinal cross-section of a CF filament (*a*), an optical microscopy image of the transverse cross-section of a CF filament (*b*), a SEM image of the surface of CF filaments (*c*), an optical microscopy image of the surface of a CF filament (*d*)

radiation was used for the X-ray diffraction studies; a selectively absorbing β filter (Fe) was installed directly in front of the window detector to filter out the *K*β series. The absolute error when measuring the angular positions of the X-ray diffraction maxima did not exceed ± 0.03 deg. The interlayer spacing d_{002} was calculated from the position of the center of gravity of the (002) line using the Bragg's law, as follows [14, 15]:

$$d_{002} = \frac{n\lambda_{\text{p}}}{2\sin\vartheta}, \qquad (2)$$

where n = 1 is the reflection order; λ_{p} is the X-ray radiation wavelength; ϑ is the reflection angle determined by the geometry of recording.

The height L_{c} of crystallites was calculated from the half-width of the X-ray diffraction maxima by using the following modified Selyakov–Scherrer formula [14, 15]:

$$L = \frac{A\lambda_{\text{p}}}{\beta\cos\vartheta}, \qquad (3)$$

where β is the half-width of the (002) diffraction peak; A = 0.89 is the constant depending on the particle shape.

The X-ray diffraction lines were analyzed using the Difract software package developed at AO Nauchnye Pribory (St. Petersburg, Russia).

Microphotos of typical samples are shown in Fig. 1. To reduce the influence of the orientation of filaments on the intensity of the (002) diffraction maximum, CF strands were preliminarily crushed in a Fritsch agate ball mill for 15 minutes until reaching the length-to-diameter ratio of the obtained particles in the range from 1 to 7. (see Fig. 1*c* and *d*). The grinding time was chosen in such a way that the variation of the (002) diffraction peak intensity during the packing of a powdered sample would be reduced [16].

Results and discussion

Figure 2 displays the Raman spectra of the surface of filaments of CFs obtained at different HTT. The spectra are typical of all classes of carbon materials and display the major tendency of the growth of the crystalline structure order with the increase of the HTT: the I_D/I_G parameter increases with the increase of the HTT above 2000 °C; the 2D spectral line, usually having a sophisticated shape, appears [17–24]. The shape of the peaks, as well as the tendency for change of the spectral characteristics, with the rise in the HTT, correlate with the known literature data [17–20]. However, when interpreting the Raman spectra of CFs, it is advisable to consider their specific crystalline structure, well studied with the X-ray diffraction and electron microscopy methods [1, 12, 17, 25, 26].

Polyacrylonitrile is a linear polymer which cyclization begins at the destruction of the source polymer via thermal oxidation with oxygen at temperatures 170–300 °C [1–4]. High-strength CFs are obtained after the carbonization of thermally oxidized PAN-fibre at temperatures 1200–1500 °C, when the crystalline structure of CFs has formed. However, at this stage the crystallites have small sizes (1–3 nm) with a relatively low degree of orientation of graphene layers relative to the fibre axis [1–5]. The average misalignment angle relative to the fibre axis for high-strength CFs is 20–30° [1–5, 12, 17, 25].

High-modulus CFs were obtained after the graphitization stage (2200–3000 °C) during which the structure of carbonized fibre changed: the degree of perfection of crystalline structure of CF rose; the interlayer spacing decreased, the crystalline size increased, while the degree of alignment of graphene layers relative to the fibre axis increased. With the increase of HTT and drawing rate the average misalignment angles relative to the fibre axis decreased to 12–16° [1–5, 12, 17, 25]. It is the growth of crystallite sizes and the increase in the degree of their alignment that determines the high Young modulus values of the obtained CFs [1–5].

The relations displayed in Figure 3*a* show that with the rise in the HTT from 1290 to 3150 °C the I_D/I_G parameter decreases from 2.9 to 0.2, which correlates with the literature data [17–18, 20]. According to formula (1), this relation corresponds to the process of the growth of crystalline sizes $L_{a\parallel}$, located on the surface of CF filaments.

Figure 3*b* shows the results of the investigation of the relationship between the values L_a obtained from the X-ray diffraction method with the I_D/I_G parameter. It can be seen that for PAN-based CFs with different processing temperatures the I_D/I_G parameter measured on the surface of filaments by different investigators, correlates well with crystalline sizes L_a, which validates the Tuinstra-Koenig Relation (1) for L_a sizes above 2 nm [7, 13, 27, 28]. For the L_a sizes below 2 nm, the values of the I_D/I_G parameter were determined by the concentration of defects and, according to [7, 27–28], were proportional to L_a^2 (see Fig. 3*b*).

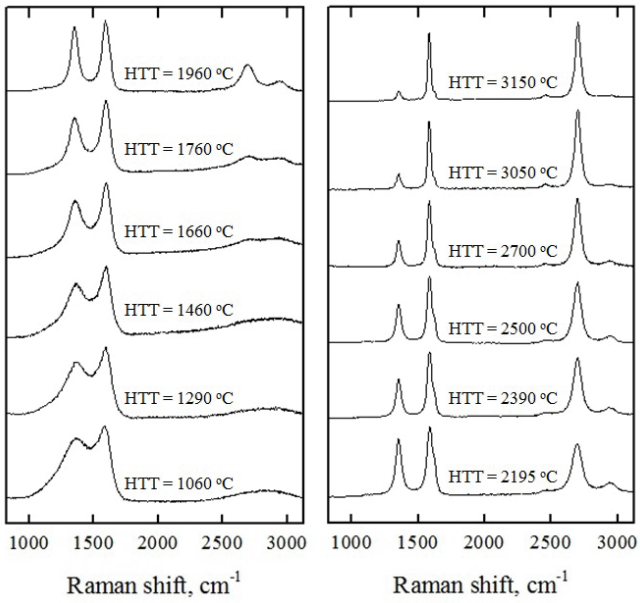

Fig. 2. Raman spectra of the surface of PAN-based CF filaments obtained at different heat treatment temperatures

It is worth noting that there existed a strong correlation between the I_D/I_G parameter and other X-ray diffraction structural parameters – interlayer spacing d_{002} and crystallite height L_c, as can be seen from Figures 3*c* and 3*d*. As can be seen, the interlayer spacing d_{002} changed from 0.342 to 0.365 nm; the crystallite height L_c increased from 2 nm to 8.2 nm. It is worth noting that our experimental data correlate well with literature data [17, 20, 30–32].

Figure 4 shows the Raman spectra of a high-strength CF (HTT = 1660 °C) compared to the Raman spectra of a high-modulus CF (HTT = 3050 °C), taken from the surface, longitudinal and transverse cross-sections of filaments. Figure 4 is complimented with the values of the I_D/I_G parameter and the corresponding values of $L_{a\parallel}^R$ for the filament surface and L_a^R for the longitudinal and transverse cross-sections of filaments, obtained from the relation (1).

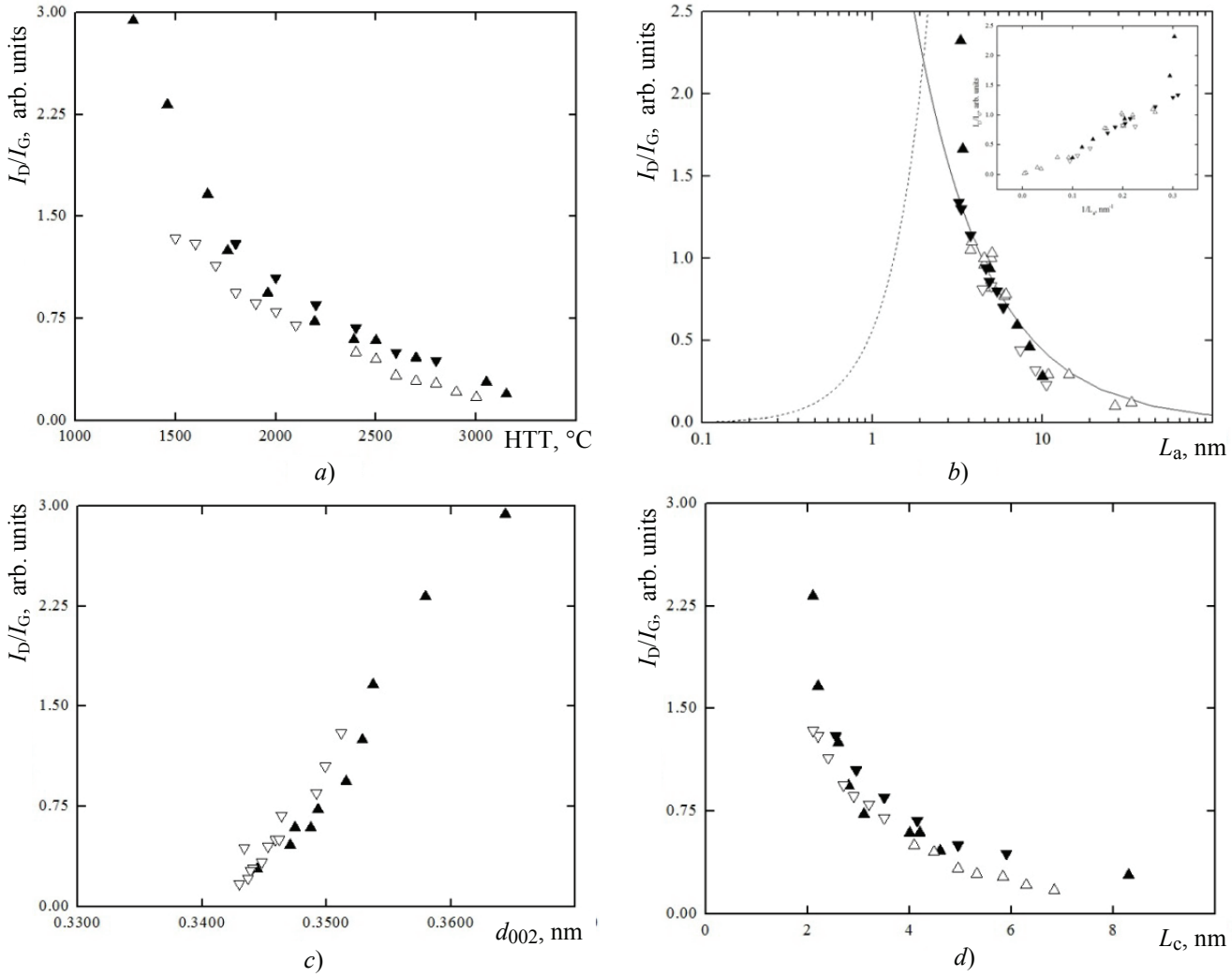

Fig.3. The relation between the I_D/I_G parameter and heat treatment temperature and PAN-based CF crystalline structure parameters:

a – the relation between the I_D/I_G parameter and CF heat treatment temperature ranging from 1290 to 3150 °C;

b – the correlation between the values of L_a obtained from the X-ray diffraction method and the I_D/I_G parameter (Solid line – the Tuinstra-Koenig relation $I_D/I_G \sim L_a^{-1}$; Broken line – $I_D/I_G \sim L_a^{2}$; On the inset – the relation between the I_D/I_G parameter and the values of L_a^{-1} obtained from the X-ray diffraction method);

c – the correlation between the I_D/I_G parameter and interlayer spacing d_{002};

d – the correlation between the I_D/I_G parameter and crystallite height L_c;

▲ – experimental data; △ – [17] data; ▽ – [18] data; ▼ – [20] data (*a*, *d*);

▲ – experimental data; △ – [6] data; ▽ – [12] data; ▼ – [18] data (*b*, *c*)

It can be seen that the spectral characteristics of the investigated CFs differ. For the high-strength CF (see Fig. 4*a*), the values of the I_D/I_G parameter taken from different positions on the filaments, and the corresponding values of $L_{a\|}^R$ and L_a^R, differ only slightly from each other, and increased from 1,75 to 2,15 arb. units and from 2.0 to 2.5 nm, respectively. These data confirm the known literature [1–4] conception about the high degree of perfection of the crystalline structure of PAN-based high-strength CFs.

On the other hand, the crystalline structure of high-strength CFs demonstrated significant heterogeneity: the surface possessed a much higher degree of perfection, and, consequently, larger crystallite sizes, than the centre of filaments; the crystallite sizes in the cross-section varied slightly, however, the spectrum taken from the periphery of the longitudinal cross-section corresponded to a higher degree of perfection of the crystalline structure, and, consequently, larger crystalline sizes, than the spectrum

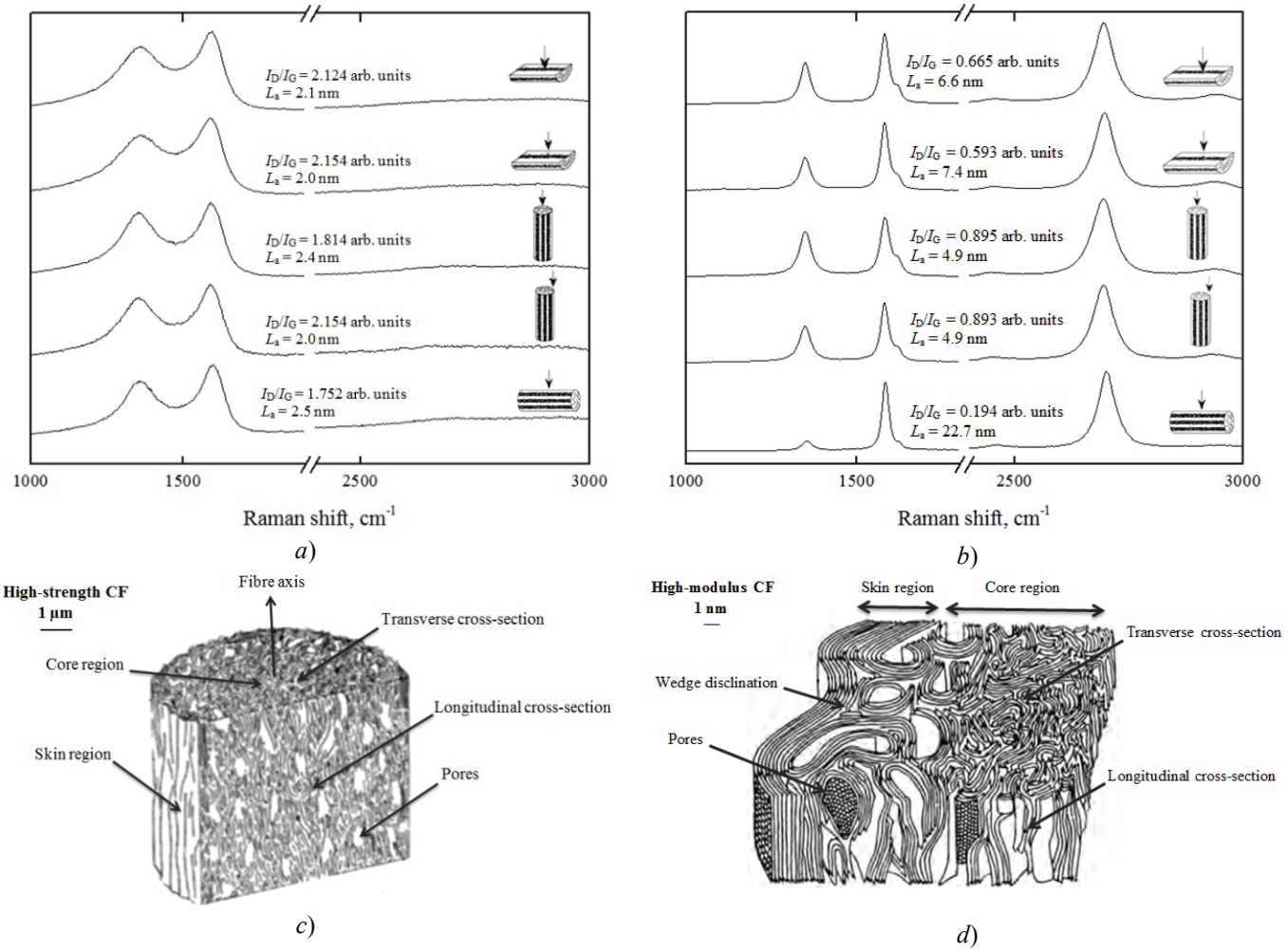

Fig. 4. Raman spectra of high-strength and high-modulus CFs taken from the surface and longitudinal and transverse cross-sections of filaments and structural models of high-strength and high-modulus PAN-based CFs proposed by Bennett and Johnson and co-authors [1, 26]:

a – high-strength CF (HTT = 1660 °C); *b* – high-modulus CF (HTT = 3150 °C); *c* – structural model of high-strength CF [1]; *d* – structural model of high-modulus CF [26]

taken from the central part of the longitudinal cross-section of the filament (see Fig. 4*b*). The crystallite sizes L_a^R in the longitudinal and transverse cross-sections varied from 4.9 to 7.4 nm; the crystallite sizes $L_{a\parallel}^R$ on the surface of filaments were much higher and reached 22.7 nm.

It is worth noting that the obtained data wholly validates the adequacy of the structural models proposed by Johnson and co-authors [1, 26], displayed in Figs 4*c* and 4*d*.

Figure 5 shows the relations between HTT and the I_D/I_G parameters, measured on the surface and the central part of the longitudinal cross-section of CF filaments. As mentioned above, calculations from Formula (1) give us the relations between $L_{a\parallel}^R$ and L_a^R, measured on the surface and the centre of the longitudinal cross-section of filaments, and HTT. Figure 5 is complimented with the values of L_a^R, calculated from literature data [20], as well as the values of L_a obtained from the X-ray diffraction method.

The relations displayed in Figure 5 show that for high-strength CFs, processed at temperatures around 1300–1500 °C, there was no significant difference in the values of $L_{a\parallel}^R$ and L_a^R, and L_a. For high-modulus CFs obtained at 2000–3000 °C, there was significant variation between the above parameters.

For such CFs, the $L_{a\parallel}^R$ values appear to be higher, and the L_a^R values lower than the values of L_a obtained from the X-ray diffraction method.

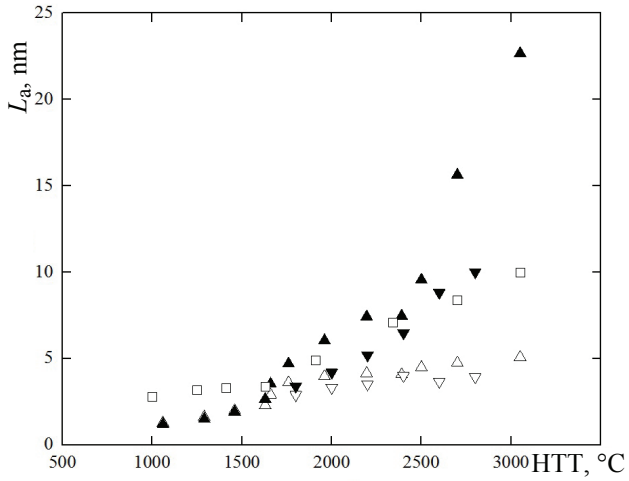

Fig. 5. The relation between the crystallite sizes measured with the X-ray diffraction method (L_a)and obtained from the corresponding I_D/I_G parameters ($L_{a\parallel}^R$ for the surface of filaments and L_a^R for the center of the transverse cross-section of filaments) and PAN-based CF heat treatment temperature:

□ – L_a (experimental data);

△ – $L_{a\parallel}^R$ (experimental data); ▽ – $L_{a\parallel}^R$ [20] data;

▲ – L_a^R (experimental data); ▼ – L_a^R [20] data

Thus, it can be deduced that the X-ray diffraction parameters display averaged values of crystallite sizes, whilst the values obtained from the Raman spectra correspond to local values of crystallite sizes for the corresponding filament parts.

According to X-ray diffraction and Electron microscopy data [33], high-modulus CF crystallites possess an elongated form; their sizes along the fibre axis L_a post-processing at temperatures 2500–3000 °C (usually with drawing) reach 20 nm, while the longitudinal values of L_a reach 10 nm, which corresponds to our experimental data.

Moreover, the relations displayed in Figure 5 act as an additional validation of the conclusions of earlier works [1, 20] that at the graphitization stage of PAN-based CFs, accompanied by the increase of the degree of alignment of crystallites relative to the fibre axis, the speeds of the crystallite growth at different CF filament parts differ: maximal on the periphery of filaments and minimal in their centre.

Conclusions

Having examined the PAN-based CFs processed at temperatures 1290–3150 °C, the Tuinstra-Koenig relation, establishing the interrelation between crystallite size and the ratio of the integral intensities of the D and G spectral bands was verified.

With the use of the Raman spectroscopy method, an independent validation of the adequacy of the early structural models of high-strength and high-modulus CFs proposed by Bennett and Johnson, was obtained.

With the use of the Raman spectroscopy method the crystallite sizes for PAN-based CFs were obtained; the relations between the crystallite sizes measured on the surface and the centre of CF filaments were derived; it was shown that with the rise of the HTT the crystallite growth on the periphery occurs approximately 5 times faster than in the centre of CF filaments.

References

1. Morgan P. *Carbon fibers and their composites*. London/Taylor and Francis. 2005. 1166 p.

2. Frank E., Steudle L.M., Ingildeev D., Spörl J.M., Buchmeiser M.R. ChemInform. Carbon Fibers: Precursor Systems, Processing, Structure, and Properties. *Angew Chem. Int. Ed Engl*, 2014, vol. 53, issue 21, pp. 5262-5298.

3. Park S.J. Carbon fibers. *Springer Series in Materials Science*, vol. 210, Springer Netherlands, 2015, pp. 330.

4. Newcomb B.A. Processing, structure, and properties of carbon fibers. *Composites Part A: Applied Science and Manufacturing*, 2016, vol. 91, Part 1. pp. 262-282, doi: http://dx.doi.org/10.1016/j.compositesa.2016.10.018

5. Varshavsky V.Y., Mayanov E.P., Sviridov A.A., Gaberling A.V. Poliakrilonitril'niye volokna i uglerodniye materialy na ikh osnove kak nanostructurirovanniye materialy. [Polyacrylonitrile fibers and polyacrylonitrile-based carbon fibers as nanostructured materials]. *Kompozity i nanostruktury* [Composites and Nanostructures], 2009, issue 4, pp. 19-27. (Rus)

6. Tuinstra F., Koenig J.L. Raman spectrum of graphite. *The Journal of Chemical Physics,* 1970, vol. 53, pp. 1126-1130.

7. Ferrari A.C., Robertson J. Interpretation of Raman spectra of disordered and amorphous carbon. *Physical review*, 2000, vol. 61, issue 20, pp. 95-107.

8. Reich S., Thomsen C. Raman spectroscopy of graphite. *Phil. Trans. R. Soc. Lond*., 2004, vol. 362, pp. 2271-2288.

9. Cançado L.G., Takai K., Enoki T., Endo M., Kim Y.A., Mizusaki H., Jorio A., Coelho L.N., Magalhães Paniago R., Pimenta M.A. General equation for the determination of the crystallite size La of nanographite by Raman spectroscopy. *Appl. Phys. Lett*., 2006, vol. 88, pp. 3106-3109.

10. Dresselhaus M.S., Dresselhaus G. Avouris Ph. *Carbon Nanotubes: Synthesis, Structure, Properties and Applications. Topics in Applied Physics (Book 80)*, Springer, 2001, pp. 477.

11. Tuinstra F., Koenig J.L. Characterization of Graphite Fiber Surfaces with Raman Spectroscopy. *Journal of Composite Materials*, 1970, vol. 4, pp. 492-499.

12. Huang Y., Young R. J.. Effect of fibre microstructure upon the modulus of pan- and pitch-based carbon fibres. *Carbon*, 1995, vol. 33, issue 2, pp. 97-107.

13. Haruki Okuda, Robert J. Young, Daniel Wolverson, Fumihiko Tanaka, Go Yamamoto, Tomonaga Okabe. Investigating nanostructures in carbon fibres using Raman spectroscopy. *Carbon*, 2018, vol. 130, pp. 178-184.

14. Sosedov V.P. *Svoystva konstrutsionnikh materialov na osnove ugleroda. Spravochnik* [Properties of carbon-based structural materials. Handbook]. Moscow, Metallurgiya Publ., 1975, 335 p. (Rus)

15. Langford J.I. A rapid method for analysing the breadths of diffraction and spectral lines using the Voigt function. *J. Appl. Cryst.,* 1978, vol. 11, pp. 10-14.

16. Bubnenkov I.A, Samoylov V.M., Verbetc D.B. [et al]. Patent RU №2685440. 18.04.2019. Bul. No.11.

17. Dongfeng Li, Haojing Wang, Xinkui Wang. Effect of microstructure on the modulus of PAN-based carbon fibers during high temperature treatment and hot stretching graphitization. *J Mater Sci*, 2007, vol. 42, pp. 4642-4649.

18. Qiu L., Zheng X.H., Zhu J., Su G.P., Tang D.W. The effect of grain size on the lattice thermal conductivity of an individual polyacrylonitrile-based carbon fiber. *Carbon*, 2013, vol. 51, pp. 265-273.

19. Haruki Okuda, Robert J. Young, Daniel Wolverson, Fumihiko Tanaka, Go Yamamoto, Tomonaga Okabe. Investigating nanostructures in carbon fibres using Raman spectroscopy. *Carbon*, 2018, vol. 130, pp. 178-184.

20. Fujie Liu, Haojing Wang, Linbing Xue, Lidong Fan, Zhenping Zhu. Effect of microstructure on the mechanical properties of PAN-based carbon fibers during high-temperature graphitization. *J Mater Sci*, 2008, vol. 43, pp. 4316-4322, doi: 10.1007/s10853-008-2633-y

21. Ribeiro-Soares J., Oliveros M.E., Garin C., David M.V., Martins L.G.P., Almeida C.A., Martins-Ferreira E.H., Takai K., Enoki T., Magalhães-Paniago R., Malachias A., Jorio A., Archanjo B.S., Achete C.A., Cançado L.G. Structural analysis of polycrystalline graphene systems by Raman spectroscopy. *Carbon*, 2015, vol. 95, pp. 646-652.

22. Soukup L., Gregora I., Jastrabik L., Kofifikovfi A. Raman spectra and electrical conductivity of glassy carbon. *Materials Science and Engineering, BI I*, 1992, pp. 355-357.

23. Jurkiewicz K., Pawlyta M., Zygadło D., Chrobak D., Duber S., Wrzalik R., Ratuszna A., Burian A. Evolution of glassy carbon under heat treatment: correlation structure–mechanical properties. *J Mater Sci*, 2018, vol. 53, pp. 3509-3523. https://doi.org/10.1007/s10853-017-1753-7

24. Bukalov S.S., Zubavichus Ya.V., Leites L.A., Sorokin A.I., Kotosonov A.S. Structural changes in industrial glassy carbon as a function of heat treatment temperature according to raman spectroscopy and X-ray diffraction data. *Nanosystems: Physics, Chemistry, Mathematics*, 2014, vol. 5 (1), pp. 186-191.

25. Oskar Paris, Dieter Loidl, Herwig Peterlik. Texture of PAN- and pitch-based carbon fibers. *Carbon*, 2002, vol. 40, pp. 551-555.

26. Bennett S.C., Johnson D.J., Johnson W. Strength-structure relationships in PAN-based carbon fibres. *Journal of materials science*, 1983, vol. 18, pp. 3337-3347.

27. Zickler G. A., Smarsly B., Gierlinger N., Peterlik H., Paris O. A reconsideration of the relationship between the crystallite size La of carbons determined by X-ray diffraction and Raman spectroscopy. *Carbon*, 2006, vol. 44, pp. 3239-3246.

28. Cancado L.G., Jorio A., Martins Ferreira E.H., Stavale F., Achete C.A., Capaz R.B., Moutinho M.V.O., Lombardo A., Kulmala T.S., Ferrari A.C. Quantifying Defects in Graphene via Raman Spectroscopy at Different Excitation Energies. *Nano Letters*, 2011, vol. 11, pp. 3190-3196.

29. Takaku A., Shioya M. X-ray measurements and the structure of polyacrylonitrile – and pitch-based carbon fibres. *Journal of Materials Science*, 1990, vol. 25, pp. 4873-4879.

30. Fisher L., Ruland W. The Influence of Graphitization on the Mechanical Properties of Carbon Fibers. *Colloid and Polymer Science*, 1980, vol. 258, pp. 917-922.

31. Watt W., Johnson W. *Appl. Polym. Symp*. 1969, vol. 9, pp. 215-227.

32. Johnson D.J. *International Conference on Carbon Fibres – their Composites and Applications*, Paper no. 8. The Plastic Institute, London, 1971.

33. Guigon M. Microtexture and Mechanical Properties of Carbon Fibers: Relationship with the Fiber-Matrix: Adhesion in a Carbon-Epoxy Composite. *Polymer Engineering and Science*, 1991, vol. 31, issue 17. https://doi.org/10.1002/pen.760311706